Complete description of all self-similar models driven by Lévy stable noise

Aleksander Weron* and Krzysztof Burnecki
Hugo Steinhaus Center, Institute of Mathematics, Wroclaw University of Technology, Wyb. Wyspianskiego 27, 50-370 Wroclaw, Poland

Szymon Mercik and Karina Weron
Institute of Physics, Wroclaw University of Technology, Wyb. Wyspianskiego 27, 50-370 Wroclaw, Poland
(Received 5 November 2003; revised manuscript received 6 May 2004; published 12 January 2005)

A canonical decomposition of H-self-similar Lévy symmetric α-stable processes is presented. The resulting components completely described by both deterministic kernels and the corresponding stochastic integral with respect to the Lévy symmetric α-stable motion are shown to be related to the dissipative and conservative parts of the dynamics. This result provides stochastic analysis tools for study the anomalous diffusion phenomena in the Langevin equation framework. For example, a simple computer test for testing the origins of self-similarity is implemented for four real empirical time series recorded from different physical systems: an ionic current flow through a single channel in a biological membrane, an energy of solar flares, a seismic electric signal recorded during seismic Earth activity, and foreign exchange rate daily returns.

DOI: 10.1103/PhysRevE.71.016113 PACS number(s): 02.50.−r, 05.40.−a, 05.20.−y, 05.45.−a

I. INTRODUCTION

The importance of Lévy stable distributions or processes in physics and related areas has long been known [1–7]. They are also increasingly important in many other fields of application. Consequently, a general trend nowadays is to put Lévy stable type anomalous diffusion on a similar footing with Brownian diffusion [8–18]. However, in what concerns our understanding of a structure of their self-similarity, the situation is vastly different for the two types of models.

At the level of the Langevin equation the Lévy motion is a generalization of the Brownian one which describes the motion of small macroscopic particles in a liquid (or a gas) experiencing unbalanced bombardments due to surrounding atoms. The Brownian motion mimics the influence of the "bath" of surrounding molecules in terms of a mean-field, time-dependent stochastic force which is commonly assumed to be white Gaussian noise. That postulate is compatible with the assumption of a short correlation time of fluctuations (much shorter than the time scale of the macroscopic motion) and the assumption of weak interactions with the bath. In contrast, the Lévy motions describe results of strong collisions between the test particle and the surrounding environment, and hence, lead to models of the bath that go beyond the standard "close-to-equilibrium" Gaussian description. The already observed unusual statistical properties of systems driven by them serve as a challenge for generalizations of thermostatics trying to explain the non-Gibbsian phenomena [2,4,5].

The notion of self-similarity, originally coined by Mandelbrot, has been introduced in 1962 by Lamperti [19]. Historically oldest approach to self-similarity has been proposed by Kolmogorov in 1940, who introduced fractional Brownian motion, which is a Gaussian self-similar process with stationary increments. For the details see Mandelbrot and Van Ness [20] and references therein. The study of non-Gaussian self-similar processes with stationary increments was initiated by Taqqu [21]. He addressed the question what type of limiting distributions is expected to appear if the stationary sequence has a stronger dependence violating the validity of central limit theorem, and further developed a non-Gaussian limit theorem originated by Rosenblatt. On the other hand, the works of Sinai and Dobrushin in the field of statistical physics appeared independently in the same time [22]. Since the self-similar processes such as Brownian, fractional Brownian, Lévy stable and fractional Lévy stable motion are stochastic processes that are invariant in distribution under suitable scaling of time and space, so these processes are closely related to the notion of renormalization in statistical and high energy physics.

A significant difference between Gaussian and Lévy stable distributions is that the latter have heavy tails and their variance is infinite. This means that much larger jumps or flights are possible for Lévy stable distributions, which causes their variance to diverge. Since many natural processes follow Lévy stable distributions [2,23–25], the necessity of modeling physical phenomena with heavy tailed distributions is dramatically increasing in many fields of physics. In this paper we employ ergodic theory foundation of ubiquity of Lévy stable self-similar processes in physics and provide a catalog of models for anomalous diffusion [2–6]. To be more precise we develop tools for study of diffusion processes described by the following Langevin-type stochastic differential equation driven by Lévy stable noise:

$$dX_t = b(t,X_t)dt + \sigma(t,X_t)dZ_t^{\alpha}, \tag{1}$$

where dZ_t^{α} stands for the increments of Lévy α-stable motion Z_t^{α}, $0<\alpha\leqslant 2$; see [25].

Section II starts with time and scale invariance of self-similar processes. Two basic examples: fractional Brownian motion and fractional Lévy stable motion are described there in the form of stochastic integrals. Also a connection with

*Electronic address: aleksander.weron@pwr.wroc.pl

long-memory or long-range dependence is established. In Sec. III we provide a theoretical justification of the recently proposed Burnecki, Mercik, Weron, and Weron (BMW^2) computer test [26] introduced to detect the origins of the self-similarity feature of a particular model. Thus it follows that the estimated index of self-similarity can reflect a long-memory effect or infinite variance impact of the process. In Sec. IV we discuss the integral representation of Lévy stable self-similar processes in the language of nonsingular flows and exploit the connection with the Hopf decomposition. This gives a natural physical interpretation of the Burnecki, Rosinski, and Weron (BRW) decomposition introduced in [27]. We identify the three components of the BRW decomposition with mixed fractional motion, harmonizable and evanescent processes, respectively. The first process corresponds to a dissipative part and two others to a conservative part of the dynamics given by the nonsingular flow representing a Lévy stable and self-similar process. A number of special examples is discussed in details in order to demonstrate that the proposed integral representation is user-friendly and could provide new insights into the mechanism underlying a range of natural phenomena. Finally, in Sec. V the obtained results are applied to determine basic features of an empirical data series. We demonstrate this by studying four empirical time series recorded from different physical systems: an ionic current flow through a single channel in a biological membrane, an energy of solar flares, a seismic electric signal recorded during seismic Earth activity, and foreign exchange (FX) rate daily returns.

II. SELF-SIMILARITY OF FRACTIONAL LÉVY STABLE MOTION

Over the past decade there has been much interest in the asymptotic behavior of dynamical systems, in particular in detecting self-similar character of these systems and testing for the existence of so-called "long memory" or "long-range dependence." It turns out that the self-similar processes are very important mathematical objects which can be used to model many physical, geophysical, hydrological, economical, and biological phenomena (see [16–18,22,28–38] and references therein). The mathematical constructions were successfully used to model diffusion on fractals, currency and stock market prices, ionic current flow through a single channel in a biological membrane, turbulences, communication and many others. Since the self-similarity property was observed in many real phenomena there is a need to build efficient estimators of the self-similarity index [30,31,38].

A self-similar stochastic process is a process that is invariant under suitable translations of time and scale. We mention that the self-similarity is described by a real positive parameter $H>0$ called self-similarity index which provides information on the investigated time series structure, correlations and fractal properties. For example, the Brownian motion is self-similar with $H=1/2$; it has no memory and its increments have finite variance.

It is well known that if a process has purely random increments with infinite variance then the process can be self-similar with index of self-similarity different from $1/2$. An example of $H=1/\alpha$ self-similar process is the Lévy stable motion with stationary and independent, identically distributed increments with symmetric α-stable distribution [25,37]. When one applies to that process the R/S analysis, the obtained Hurst exponent equals $1/2$ since the estimator shows a lack of memory [26]. Thus the second origin of the self-similarity is the process' increments distribution what is, to our knowledge, neglected by many authors. There is another example of even more complicated process—the fractional Lévy stable motion [25,37] which has the memory property and increments with infinite variance. In this case the self-similarity index carries information on both, on long-memory and increments distribution. Hence studying the process' self-similarity one needs to have robust statistical tools and clear algorithms to extract information on both of the factors. A simple hint is as follows: if one wants to investigate the self-similarity property, one needs to distinguish between the long-memory property and the process' increments distribution properties. Otherwise a wrong conclusion can be drawn. In [26] we provided an explicit algorithm distinguishing between the origins of the self-similarity in the case of a given time series on the base of a simple simulation experiment (computer test).

A. Self-similar processes

As we mentioned above, the self-similar processes are the ones that are invariant under suitable translations of time and scale. They are important in probability theory because of their connection to limit theorems and they are of great interest in modeling heavy-tailed and long-memory phenomena. In fact, Lamperti used the term "semi-stable" in order to underline that the role of self-similar processes among stochastic processes is analogous to the role of stable distributions among all distributions.

A process $\{X(t)\}_{t\geqslant 0}$ is called self-similar [19] if for some $H>0$,

$$X(at) \overset{d}{=} a^H X(t) \quad \text{for every } a>0, \tag{2}$$

where $\overset{d}{=}$ denotes equality of all finite-dimensional distributions of the processes on the left and right. The process $X(t)$ is also called an H-self-similar process and the parameter H is called the self-similarity index or exponent. If we interpret t as "time" and $X(t)$ as "space" then Eq. (2) tells us that every change of time scale $a>0$ corresponds to a change of space scale a^H. The bigger H, the more dramatic is the change of the space coordinate.

Notice that Eq. (2), indeed, means a "scale-invariance" of the finite-dimensional distributions of $X(t)$. This property of a self-similar process does not imply the same for the sample paths. Therefore, pictures trying to explain self-similarity by some zooming in or out on one sample path, are by definition misleading. Why? In contrast to the deterministic self-similarity, the self-similarity of stochastic processes does not mean that the same picture repeats itself exactly as we go closer. It is rather the general impression that remains the same. A convenient mathematical tool to observe self-similarity is provided by so-called quantile lines [25].

Many of the interesting self-similar processes have stationary increments. A process $\{X(t)\}_{t\geqslant 0}$ is said to have stationary increments if for any $b>0$,

$$[X(t+b)-X(b)] \stackrel{d}{=} [X(t)-X(0)]. \tag{3}$$

B. Fractional Brownian motion

The fractional Brownian motion (FBM) $\{B_H(t)\}_{t\geqslant 0}$ has the integral representation

$$B_H(t) = \int_{-\infty}^{\infty} [(t-u)_+^{H-1/2} - (-u)_+^{H-1/2}] dB(u), \tag{4}$$

where $x_+ = \max(x,0)$ and $B(u)$ is a Brownian motion (BM). It is H-self-similar with stationary increments and it is the only Gaussian process with such properties for $0<H<1$ [37]. The classic Brownian motion $B(t)$, used by Einstein and Smoluchowski, is simply a special case of the fractional Brownian motion when $H=1/2$.

In modeling of long-memory phenomena, the stationary increments of H-self-similar processes are of special interest since any H-self-similar process with stationary increments $\{X(t)\}_{t\in\mathbb{R}}$ induces a stationary sequence $\{Y_j\}_{j\in\mathbb{Z}}$, where $Y_j = X(j+1)-X(j)$; $j=\ldots,-1,0,1,\ldots$. The sequence Y_j corresponding to the fractional Brownian motion is called fractional Gaussian noise (FGN) [26]. It is called a standard fractional Gaussian noise if $\mathrm{var}Y_j=1$ for every $j\in\mathbb{Z}$.

The fractional Gaussian noise has some remarkable properties. If $H=1/2$, then its autocovariance function $r(k) = R(0,k)=0$ for $k\neq 0$ and hence it is the sequence of independent identically distributed (i.i.d.) Gaussian random variables. The situation is quite different when $H\neq 1/2$, namely the Y_j's are dependent and the time series has the autocovariance function of the form

$$r(k) \sim \mathrm{var}Y_1 H(2H-1)k^{2H-2}, \quad \text{as } k\to\infty. \tag{5}$$

The autocovariance function $r(k)$ tends to 0 as $k\to\infty$ for all $0<H<1$, but when $1/2<H<1$ it tends to zero so slowly that the sum $\Sigma_{k=-\infty}^{\infty} r(k)$ diverges. We say that in this case the increment process exhibits long-memory or "long-range dependence" [30]. Moreover, formula (5) by the Wiener Tauberian theorem (see [39], Chap. V 2) implies that the spectral density $h(\lambda)$ of the stationary process FGN has a pole at zero. A phenomenon often referred to as "$1/f$ noise."

If $0<H<1/2$, then $\Sigma_{k=-\infty}^{\infty} r(k)=0$ and the spectral density tends to zero as $|\lambda|\to 0$. We say in that case that the sequence displays a short-memory. Furthermore, as the coefficient $H(2H-1)$ is negative, the $r(j)$'s are negative for all large j, a behavior referred to as "negative dependence."

C. Fractional Lévy stable motion

The most commonly used extension of the fractional Brownian motion to the α-stable case is the fractional Lévy stable motion (FLSM) [40–42]. The process $\{Z_\alpha^H(t)\}_{t\in\mathbb{R}}$ is defined by the following integral representation

$$Z_\alpha^H(t) = \int_{-\infty}^{\infty} [(t-u)_+^{H-1/\alpha} - (-u)_+^{H-1/\alpha}] dZ_\alpha(u), \tag{6}$$

where $Z_\alpha(u)$ is a symmetric Lévy α-stable motion (LSM) [25,37]. The integral is well defined for $0<H<1$ and $0<\alpha\leqslant 2$ as a weighted average of the Lévy stable motion $Z_\alpha(u)$ over the infinite past with the weight given by the above integral kernel denoted by $f_t(u)$.

The process $Z_\alpha^H(t)$ is H-self-similar and has stationary increments [40]. Let us observe that H-self-similarity follows from the above integral representation and the fact that the kernel $f_t(u)$ is d-self-similar with $d=H-1/\alpha$, when the integrator $Z_\alpha(u)$ is $1/\alpha$-self-similar. This implies the following important relation:

$$H = d + \frac{1}{\alpha}. \tag{7}$$

The representation (6) of FLSM is similar to the representation (4) of the fractional Brownian motion. Therefore, FLSM reduces to the fractional Brownian motion if one sets $\alpha=2$. When we put $H=1/\alpha$ we obtain the Lévy α-stable motion which is an extension of the Brownian motion to the α-stable case. We note, that contrary to the Gaussian case ($\alpha=2$) the Lévy α-stable motion ($0<\alpha<2$) is not the only $1/\alpha$-self-similar Lévy α-stable process with stationary increments (this is true for $0<\alpha<1$ only).

The increment process corresponding to the fractional Lévy stable process is called a fractional stable noise (FSN). By analogy with the case $\alpha=2$, we say that FSN has the long-range dependence when $H>1/\alpha$ and the negative dependence when $H<1/\alpha$. If $H=1/\alpha$ the increments of FLSM are i.i.d. symmetric α-stable variables. The asymptotic dependence structure of the fractional Brownian noise is studied by virtue of the autocovariance function. Since in the α-stable case the second moment is infinite one has to use another measure of dependence, e.g., the codifference $\tau(j)$ which equals the covariance when $\alpha=2$ [37]. For most, but not all, values of α and H, τ decreases as $j^{\alpha H-\alpha}$ for large j. This is analogous to the behavior of the autocovariance function in the Gaussian case $\alpha=2$. Finally, we note that there is no long-range dependence when $0<\alpha\leqslant 1$ because H is constrained to lie in the interval (0, 1).

For simulations of the above self-similar processes we need specific computer generators. Two of such algorithms for generation of fractional Gaussian noise (FGN) and fractional stable noise (FSN) are described in detail in [26] and [43].

III. TESTING OF SELF-SIMILARITY

In this section we use the absolute value (AV) method for estimation of the self-similarity index H. The method is based on calculating mean value from the process realizations and studying its scaling with a sample length [31]. A time series of length N one divides into subseries of length m and calculates the first absolute moment

$$M_{\mathrm{AV}}^{(m)} = \frac{1}{N/m} \sum_{k=1}^{N/m} |X^{(m)}(k) - \langle X \rangle|, \tag{8}$$

where $X^{(m)}$ is an mth subseries and $\langle X \rangle$ is the overall series mean.

The obtained statistics scales with the window size and the absolute value exponent A equals $H_{\mathrm{AV}}-1$, where H_{AV} is the self-similarity index

$$M_{\mathrm{AV}}^{(m)} \propto m^{H_{\mathrm{AV}}-1}. \tag{9}$$

Notice, that this estimator gives information on the self-similarity index. If the variance of the time series is infinite the estimator also works correctly, so it can be used to investigate, for example, the Lévy stable motion.

To investigate memory of a studied process we apply the estimator to an original data set obtained as a realization of the process given by Eq. (6) and to the surrogate data. Surrogate data refers to data that preserve certain linear statistic properties of the experimental time series, without the deterministic component [44]. It is commonly used to determine the memory of a process by means of the local dispersion and nonlinear prediction methods. The surrogate data can be obtained by several different ways [44,45]. In this paper we obtain it by random shuffling of the original data positions.

According to [26] we have the following BMW^2 computer test.

If the self-similarity results from the process memory only (e.g., fractional Brownian motion) then the values of the applied estimator should change to $1/2$ for the surrogate data independently on the initial values.

If the self-similarity results only from the process' increments infinite variance (e.g., Lévy stable motion) then the estimator values should be the same for the original and surrogate data.

The self-similarity resulting from both origins (e.g., fractional Lévy stable motion) should be observed as a partial change in the estimators values.

In order to justify the above test the behavior of the estimator was investigated on simulated time series. The calculations were performed for two cases: fractional Lévy stable motion for $\alpha=1.8$ and the self-similarity index H taking values {0.6, 0.7, 0.8, 0.90} (Fig. 1 depicts sample paths of corresponding fractional stable noises for $H=0.6$ and $H=0.9$) and Lévy stable motion with the self-similarity index H taking values {0.6, 0.7, 0.8, 0.9}. The index of stability α in the latter case ranges from $\alpha=10/9$ to $\alpha=5/3$.

We note that in order to simulate fractional Lévy stable motion we directly applied its integral representation given by Eq. (18) for $t=1/100, 2/100, \ldots, 9999/100, 100$ (10000 observations). The fractional Lévy stable motion was also considered and simulated in [43].

The AV estimator calculated for every given case of the fractional Lévy stable motion and Lévy motion is presented in Fig. 2. The AV estimator gives information on both, the memory and distribution of the investigated process. The values of the estimator should form the line $A=H-1$. It is true in both studied cases, cf. circles and dashed lines in Fig. 2. The estimator values for the surrogate data obtained from fractional Lévy stable motion and Lévy motion are markedly different. In the case of the fractional Lévy stable motion values of the estimator are close to $1/1.8-1 \sim -0.44$, cf. plus signs and dotted line in Fig. 2. The values obtained for the Lévy stable motion do not change after shuffling and are pretty close to the value 1 subtracted from the self-similarity index value H, cf. plus signs and dashed line in Fig. 2.

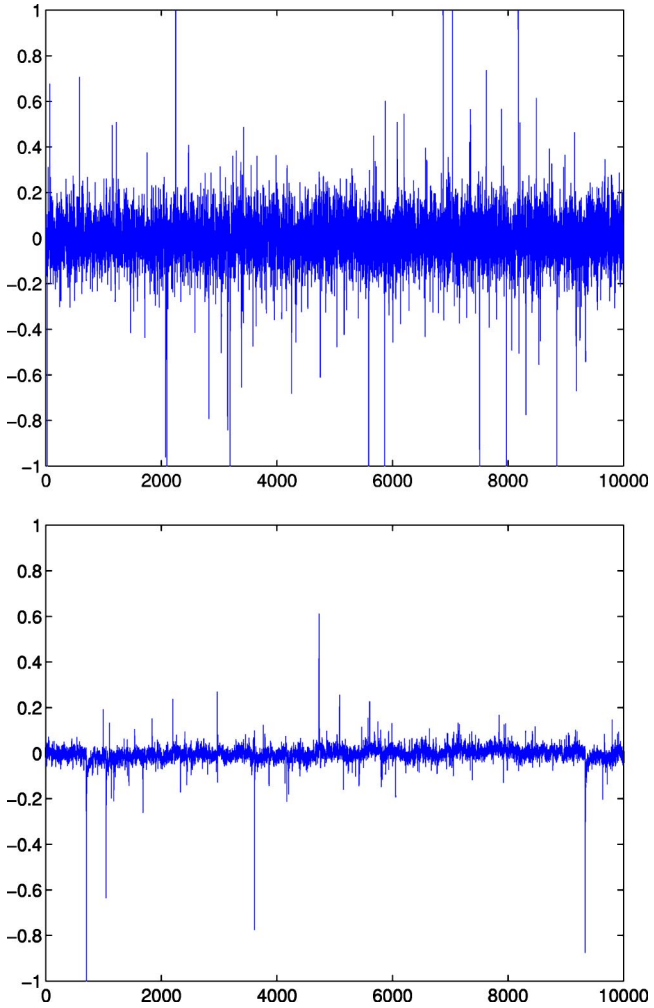

FIG. 1. A sample path of the fractional Lévy stable noise for (top panel) $H=0.6$ and $\alpha=1/1.8$, and (bottom panel) $H=0.9$ and $\alpha=1/1.8$.

IV. RELATION TO THE BRW DECOMPOSITION

In this section we exploit the connection between theory of self-similar Lévy stable processes and ergodic theory of nonsingular flows. We use the integral representation of an H self-similar (SS) symmetric α-stable (SαS) process $\{X_t\}_{t>0}$ of the form

$$X_t = \int_S f_t(u) dZ_\alpha(u), \quad t > 0, \tag{10}$$

where the kernel $f_t(u)=t^H[a_t(u)f(\phi_t(u))]m_t(u)^{1/\alpha}$ is represented by means of the tools used in ergodic theory [46]. Here $\{\phi_t\}_{t>0}$ is a nonsingular multiplicative flow on the

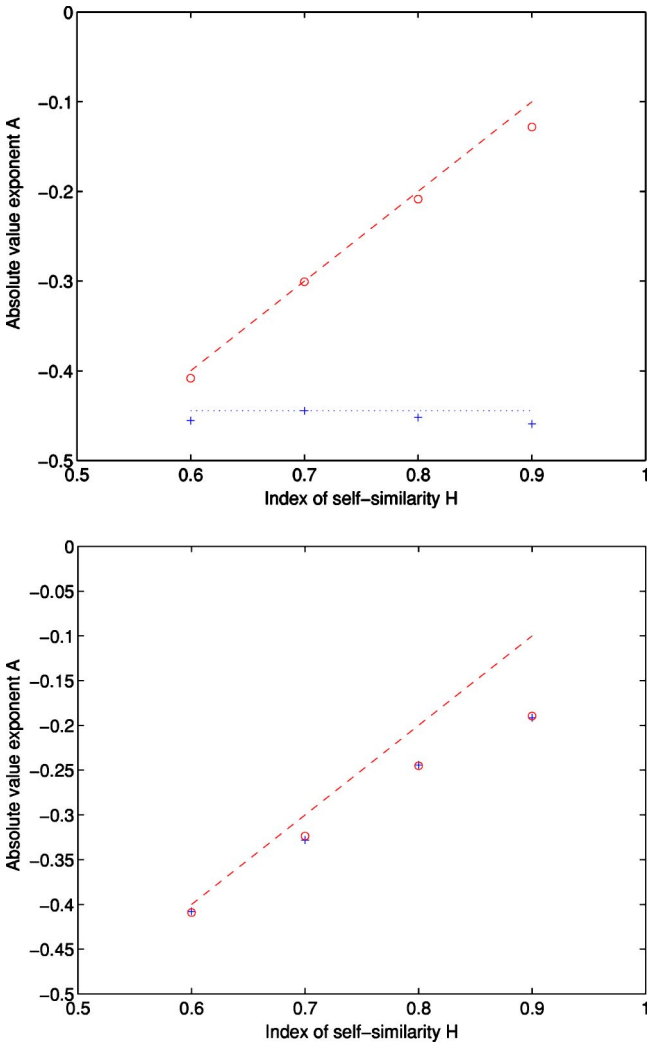

FIG. 2. Values of the AV exponent $A=H_{\mathrm{AV}}-1$ for the original time series (circle) and the surrogate data (plus sign) of (top panel) the fractional Lévy stable noise and (bottom panel) the Lévy stable noise.

phase space (S,μ), $\{a_t\}_{t>0}$ is a cocycle for this flow taking values in $\{-1,1\}$, $m_t=d(\mu(\phi_t))/d\mu$ and f is α-integrable with respect to μ [27].

The stochastic process X_t defined in Eq. (10) can be interpreted, similarly as in Sec. II, as a weighted average of the Lévy stable motion $Z_\alpha(t)$ over the infinite past with the weight given by the kernel f_t. For the exact definition we refer the interested reader to [25,37]. Let us point out that the stochastic integral (10) is equivalent to the diffusion without drift (i.e., $b=0$) and with diffusion coefficient ($\sigma=f_t$); see Eq. (1).

The self-similarity property of the above integral with parameter H, follows directly from $1/\alpha$-self-similarity of the process $Z_\alpha(t)$ and the following property of the kernel

$$f_{ct}(u)=c^{H-1/\alpha}f_t\left(\frac{u}{c}\right). \tag{11}$$

It was demonstrated in [27] that every SαS self-similar process $\{X_t\}_{t>0}$ admits a unique BRW decomposition into three independent parts

$$\{X_t\}_{t>0}\overset{d}{=}\{X_t^{(1)}\}_{t>0}+\{X_t^{(2)}\}_{t>0}+\{X_t^{(3)}\}_{t>0}, \tag{12}$$

where the first process on the right-hand side is a mixed fractional motion (MFM), the second is harmonizable, and the third one is an H SS evanescent process.

The Hopf decomposition in ergodic theory of the phase space S of the integral representation (10) into invariant parts C and D, such that the flow ϕ_t is conservative on C and dissipative on D, generates a decomposition of $\{X_t\}_{t>0}$ into two independent SαS H SS processes $\{X_t^C\}_{t>0}$ and $\{X_t^D\}_{t>0}$. The class $\{X_t^C\}_{t>0}$ generated by conservative flows consists of harmonizable processes $\{X_t^{(2)}\}_{t>0}$ and evanescent processes $\{X_t^{(3)}\}_{t>0}$. The process $\{X_t^D\}_{t>0}$ is a MFM and one can choose a minimal representation of $\{X_t^D\}_{t>0}$ of the form (14) below. Furthermore, $\{X_t^D\}_{t>0}$ is a fractional motion (FM) if and only if $\{\phi_t\}_{t>0}$ restricted to D is ergodic. This is a promising link between the BRW decomposition of any SαS H SS process and the theory of dynamical systems in statistical physics. The ergodic theory of SαS stationary processes is presented in [25]. See also [42] for the one-to-one correspondence between SαS self-similar and stationary processes.

The simplest H SS SαS process is obtained from a kernel of the form

$$f_t(s)=t^{H-1/\alpha}f\left(\frac{s}{t}\right),\quad t,s>0, \tag{13}$$

where f is α-integrable with respect to the Lebesgue measure. A SαS process with such representation is called the fractional motion. A superposition of independent FM processes of type (13) is called the mixed fractional motion and it has the form

$$g_t(w,u)=t^{H-1/\alpha}g\left(w,\frac{u}{t}\right),\quad t>0. \tag{14}$$

We will give a few examples of FM and MFM processes. We start from d-dimensional case.

Model 1. For $f\in L^\alpha(\mathbb{R}^d)$, let

$$f_t(s)=t^{H-d/\alpha}f\left(\frac{s}{t}\right),\quad s\in\mathbb{R}^d,\ t>0, \tag{15}$$

and M be a SαS random measure on $\mathbb{R}^d$ with the Lebesgue control measure. It is easy to check that a SαS process $\{X_t\}_{t>0}$ with such representation is H SS. We will show that $\{X_t\}_{t>0}$ is a MFM. Indeed, let $W=S_d$ be the unit sphere in $\mathbb{R}^d$ equipped with the uniform probability measure ν and let $g(w,u)=(c_d u^{d-1})^{1/\alpha}f(uw)$, $(w,u)\in S_d\times(0,\infty)$ where $c_d=2\pi^{d/2}/\Gamma(d/2)$ is the surface area of S_d. Using polar coordinates, we get for every $a_1,\ldots,a_n\in\mathbb{R}$, $t_1,\ldots,t_n>0$,

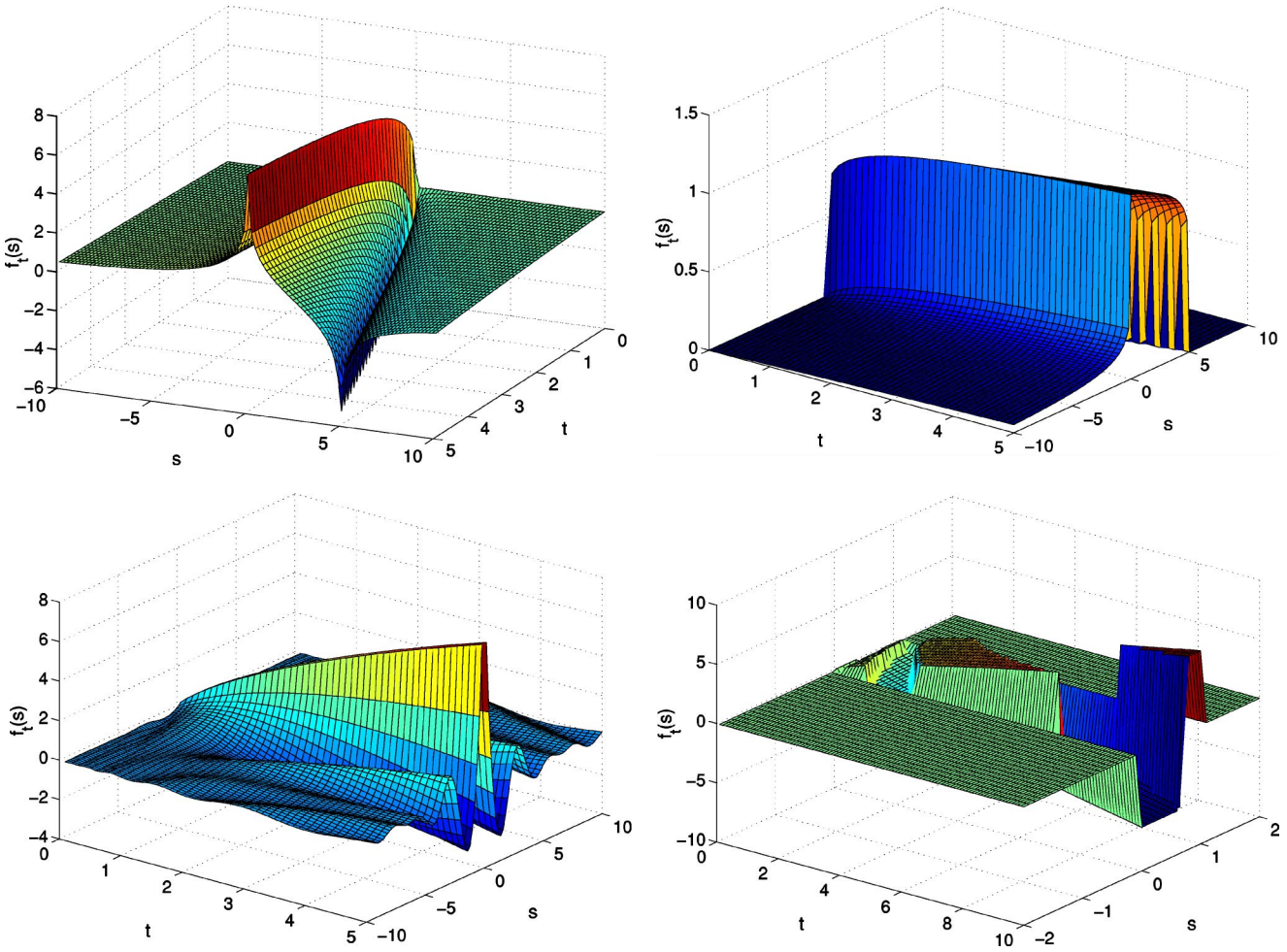

FIG. 3. The kernel of the integral representation of (top left) a log-fractional SαS motion and (top right) a fractional SαS motion for $H-1/\alpha=0.1$; (bottom left) the real part of the kernel of the integral representation of the complex-valued SαS harmonizable process for $H=0.8$ and $H-1/\alpha=0.1$ and (bottom right), the kernel of the integral representation of the evanescent process.

$$\int_{\mathbb{R}^d} \left|\sum a_j f_{t_j}(s)\right|^\alpha ds = c_d \int_{S_d}\int_0^\infty \left|\sum a_j t_j^{H-d/\alpha} f\left(\frac{uw}{t_j}\right)\right|^\alpha u^{d-1} du\,\nu(dw) = \int_{S_d}\int_0^\infty \left|\sum a_j t_j^{H-1/\alpha} g\left(w, \frac{u}{t_j}\right)\right|^\alpha du\,\nu(dw), \tag{16}$$

which proves the claim.

Comparing the kernel from the above example with the general form (10) we get that $S=\mathbb{R}^d\backslash\{0\}$, $\phi_t(s)=t^{-1}s$, $f_1(s)=f(s)$, and $d(\mu(\phi_t))/d\mu=t^{-d}$. The following well-known H SS processes are special cases of the above example.

Model 2. Let $1<\alpha<2$ and $H=1/\alpha$. Then a log-fractional SαS motion [48] $\{X_t\}_{t>0}$ is defined by the kernel

$$f_t(s) = \log|t/s - 1| \tag{17}$$

(see Fig. 3, top left).

Model 3. Let $0<H<1$, $0<\alpha<2$ and $H\neq 1/\alpha$. Put $\beta=H-1/\alpha$. Then a fractional SαS motion [49] $\{X_t\}_{t>0}$ is defined by the kernel

$$f_t(s) = I[s<0][(t-s)^\beta - (-s)^\beta] + I[0<s<t](t-s)^\beta \tag{18}$$

(see Fig. 3, top right), where $I[\cdot]$ stands for the indicator function of the s-variable.

We remark only that the Lamperti transformation [42] maps FM's onto moving average processes and MFM's onto mixed moving averages [50]. Considering above examples it seems that MFM's appear more naturally than FM's. This is quite opposite to the relation between mixed and the usual moving averages. It is clear that a Lévy stable process may have many integral representations with different kernels defined on various measure spaces. However, we can identify one property, common to all such representations, which characterizes MFM's. Let $\{X_t\}_{t>0}$ be a SαS H SS process with an arbitrary representation (10). Then X is a MFM if and only if

$$\int_0^\infty t^{-\alpha H-1}|f_t(s)|^\alpha dt<\infty \ \mu-a.e. \tag{19}$$

Observe first that this condition is equivalent to $\int_{-\infty}^{\infty}e^{-\alpha Ht}|f_{e^t}(s)|^\alpha dt<\infty \mu-a.e.$ By [47] and the Lamperti transformation this gives the result.

The class generated by conservative flows consists of harmonizable processes and processes of a third kind (evanescent). An H SS SαS process $\{X_t\}_{t>0}$ is said to be harmonizable if its kernel satisfies the condition: $f_{t_1t_2}(s)f_1(s)=f_{t_1}(s)f_{t_2}(s)$ for $t_1,t_2>0$, see [27].

A stochastic process whose minimal representation (10) contains a conservative flow without fixed points is called evanescent. This class is not well understood at present. The following result in [27] is useful to verify whether or not a process is evanescent. Let $\{X_t\}_{t>0}$ be a SαS H SS process with an arbitrary representation (10). Then $\{X_t\}_{t>0}$ is evanescent if and only if $\mu\{s\in S:\int_0^\infty t^{-\alpha H-1}|f_t(s)|^\alpha dt<\infty\}=0$ and $\mu\{s\in S:f_{t_1t_2}(s)f_1(s)=f_{t_1}(s)f_{t_2}(s) \text{ for } t_1,t_2>0\}=0$.

Finally we give examples of the harmonizable and evanescent processes.

Model 4. Let

$$f_t(s)=t^{H+is}\frac{\exp(is)-1}{is}|s|^{-(H-1+1/\alpha)} \tag{20}$$

(see Fig. 3, bottom left). It is easy to check that stochastic process with such kernel is harmonizable.

Model 5. Let

$$f_t(s)=I[0<s<1]t^H\cos(\pi\|\log t+s\|), \tag{21}$$

where $\|x\|$ denotes the largest integer not exceeding x (see Fig. 3, bottom right). Then $X(t)$ defined by the above kernel does not have a corresponding harmonizable nor mixed moving average component, so provides an example of an evanescent component.

V. EMPIRICAL EVIDENCE

The above formalism can be easily applied to determine basic features of an empirical data series. Below we demonstrate this by studying four empirical time series recorded from different physical systems: an ionic current flow through a single channel in a biological membrane, an energy of solar flares, a seismic electric signal recorded during seismic Earth activity, and FX rate daily returns.

The ionic current was recorded from cell attached patches of adult locust (Schistocerca gregaria) extensior tibiae muscle fibres [32,51,52]. The potassium current (see Fig. 4) through a high conductance locust potassium channel (BK channel) was obtained by the patch clamp technique with sampling frequency 10 kHz and at a voltage of 100 mV. The sample presents a time series, consisting of 250 000 points and covering, therefore, 25 s of recording. The error of measurements of ionic current is equal to 1 pA.

The solar flares energy data were recorded by UHURU satellite. The captured energy was transmitted by X rays emitted during blasts on a solar surface from the 1st of January 1997 to the 31st of August 2002 [53]. The time of the blast was recorded with an accuracy of 1 min and the relative error of the energy measurement reads 10^{-2}. The total analyzed sample consists of moments and energy of 13 015 flares. A part of the time series is presented in Fig. 4.

The seismic signal is a record of an electrical field of the Earth surface called SES (*Seismic Electric Signal*) [54]. The data were recorded on the 18th of April 1995 in Grevena-Kozani in Greece at the sampling frequency 1 Hz. The time series consists of 2 201 observations covering about 37 min. The measurement error reads 10 nV/km. The data are especially interesting since the SES activity usually precedes an earthquake [54]. The time series is presented in Fig. 4.

The USD/CHF FX rate was recorded from 1985-05-20 to 1991-04-12 with daily resolution. The data primarily comes from a set of financial data released by Olsen & Associates for the Second International Conference on High Frequency Data in Finance, Zürich, April 1–3, 1998. These data sets are quotations of foreign currencies and metals available from international vendors like Reuters, Knight-Ridder and Telerate. The analyzed time series consists of 1 480 observations and the daily FX rate changes are presented in Fig. 4.

The procedure presented in Sec. III (see also [26]) was applied to the above time series. The obtained values of the parameters are listed in Table I.

Comparing the values of the different estimators for the original data series and for the surrogate data one can estimate the components of the self-similarity index corresponding to the memory of the time series (d) and to the tails properties of the time series values distribution (α). The values of the components are presented in Table II. Let us observe that only for the solar flares data the self-similarity results from both origins suggesting that proper model should be based on the fractional Lévy stable motion with $H\sim 0.86$ and $\alpha\sim 1.45$, see BMW[2] computer test in Sec. III.

It is clearly seen that the procedure provides a decomposition of the self-similarity index into the two components representing memory and the tails of the process; see formula (7). Nevertheless, it is not clear how to apply the algorithm for the integral kernel (11) estimation. The difficulty mainly arises from a lack of any additional limitations for the class of functions to which can belong the kernel. So, one cannot reduce the problem of finding the kernel to a parameter or parameters estimation. Instead, one has to deal with a nonparametric estimation problem. However, having the d and α values one can already correctly classify the studied time series, identify the process $Z_\alpha(t)$ in the integral (10) and reduce the class of possible kernels. More studies are needed to elucidate the recognition of the kernel.

VI. CONCLUDING REMARKS

In this paper we demonstrate that all self-similar models driven by Lévy stable noise are completely described by formula (10) in the form of a stochastic integral with respect to the Lévy symmetric stable motion and a deterministic kernel f_t. The classical Hopf decomposition in ergodic theory implies decomposition (12) into three independent components: MFM, harmonizable and evanescent. The first component corresponds to conservative dynamics, when two others to

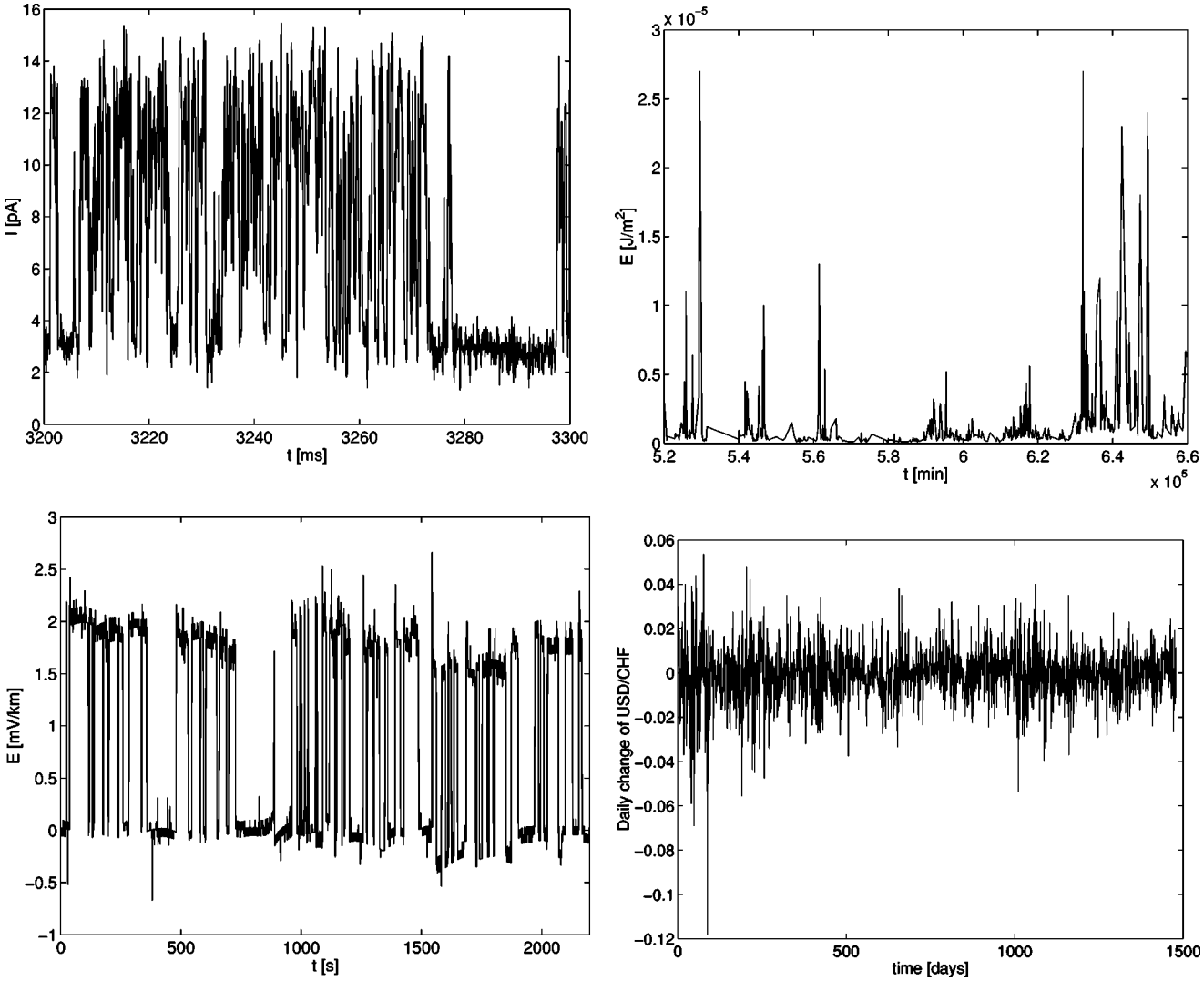

FIG. 4. A part of patch clamp recording of the single BK channel ionic current (top left); a part of solar flares energy time series (top right); seismic electric signal recorded on the 18th of April 1995 in Grevena-Kozani in Greece (bottom left); and the USD/CHF FX rate daily changes from 1985-05-20 to 1991-04-12 (bottom right).

TABLE I. Values of the Hurst and DFA exponents and the self-similarity index H_{AV} for the original time series and the surrogate data for the four different data sets.

Data set	Hurst	DFA	H_{AV}
		Original time series	
Ionic current	0.84±0.08	0.89±0.07	0.88±0.08
Solar flares	0.69±0.05	0.68±0.07	0.86±0.06
SES	0.92±0.06	0.94±0.10	0.89±0.07
FX rate	0.62±0.10	0.51±0.05	0.57±0.08
		Surrogate data	
Ionic current	0.54±0.05	0.50±0.04	0.48±0.05
Solar flares	0.52±0.04	0.48±0.05	0.69±0.06
SES	0.56±0.07	0.48±0.07	0.49±0.07
FX rate	0.60±0.10	0.50±0.05	0.54±0.07

dissipative dynamics. Next, we provide the five typical H-self-similar models and characterize the three possible components in the language of their deterministic kernels f_t.

On the level of observed physical time series this leads to a challenging open problem how to see the "shape" of the self-similarity from the data? To be more precise, how to determine the type of the model from the given time series data. Details of these ideas are, however, the subject of the current work and are beyond the scope of this paper. If one knows how to recognize the form of the kernel f_t from the data (by a shape recognition procedure), then from our result it follows that this time series corresponds to a specific part of the BRW decomposition. For instance, MFM is identified if and only if the kernel f_t satisfies condition (19).

The main findings is that always a deterministic kernel determines the index of self-similarity H via formula (11). This provides a catalog of all possible self-similar models for anomalous diffusion driven by Lévy stable noise. We also study an explicit algorithm distinguishing between the ori-

TABLE II. Values of the self-similarity index components (d,α), and the type of modeling processes for the four analyzed time series.

Data set	d	α	Modeling process
Ionic current	0.36 ± 0.08	2.00 ± 0.22	FBM
Solar flares	0.19 ± 0.07	1.45 ± 0.14	FLSM
SES	0.43 ± 0.09	2.00 ± 0.34	FBM
FX rate	0.00 ± 0.05	1.80 ± 0.20	LSM or BM

gins of the self-similarity of a given time series on the base of the BMW^2 computer test [26]. It turns out that it suffices to compare the behavior of AV estimator of H for the original time series and the surrogate data. We provide here a theoretical justification of this algorithm for self-similar models using general formula (10). This is illustrated in Sec. V for four sets of empirical data recorded from different physical systems.

ACKNOWLEDGMENTS

We are grateful to Professor P. N. R. Usherwood and Dr. I. Mellor from the University of Nottingham (UK), and to Dr. Z. Siwy from the Silesian University of Technology (Poland) for providing us with the experimental data of ion current through high conductance locust potassium channel. We are grateful to Professor P. Varotsos from the University of Athens (Greece) for providing us with the SES data. The research was partially done with the ESF Programme STOCHDYN.

[1] A. Chechkin *et al.*, Phys. Rev. E **67**, 010102(R) (2003).
[2] I. Eliazar and J. Klafter, J. Stat. Phys. **111**, 739 (2003).
[3] A. Chechkin, J. Klafter, and I. M. Sokolov, Europhys. Lett. **63**, 326 (2003).
[4] B. Dybiec and E. Gudowska-Nowak, Phys. Rev. E **69**, 016105 (2004); Fluct. Noise Lett. **4**, L273 (2004).
[5] A. Chechkin *et al.*, Chem. Phys. **284**, 233 (2002).
[6] I. M. Sokolov, J. Klafter, and A. Blumen, Phys. Today **55**, 48 (2002).
[7] H. Schiessel, I. M. Sokolov, and A. Blumen, Phys. Rev. E **56**, R2390 (1997).
[8] T. J. Penna *et al.*, Phys. Rev. E **52**, R2168 (1995).
[9] E. S. Kikkinides and V. N. Burganos, Phys. Rev. E **59**, 7185 (1999).
[10] K. I. Hopcraft, E. Jakeman, and R. M. J. Tanner, Phys. Rev. E **60**, 5327 (1999).
[11] A. V. Milovanov and L. M. Zelenyi, Phys. Rev. E **64**, 052101 (2001).
[12] B. L. Lan, Phys. Rev. A **63**, 042105 (2001).
[13] S. Picozzi and B. J. West, Phys. Rev. E **66**, 046118 (2002).
[14] M. Kotulska and A. Jurlewicz, Acta Phys. Pol. B **31**, 1085 (2000); M. Kotulska, S. Koronkiewicz, and S. Kalinowski, Phys. Rev. E **69**, 031920 (2004).
[15] S. Borelli, D. Fioretto, and A. Jurlewicz, J. Phys.: Condens. Matter **13**, 373 (2001).
[16] J. Nowicka-Zagrajek, Stoch. Models **13**, 673 (1997).
[17] J. Nowicka-Zagrajek and R. Weron, Signal Process. **82**, 1903 (2002).
[18] R. Weron, Int. J. Mod. Phys. C **12**, 209 (2001).
[19] J. W. Lamperti, Trans. Am. Math. Soc. **104**, 62 (1962).
[20] B. Mandelbrot and J. W. Van Ness, SIAM Rev. **10**, 422 (1968); B. Mandelbrot, *Fractals and Scaling in Finance* (Springer, Berlin, 1997).
[21] M. S. Taqqu, in *Dependence in Probability and Statistics*, edited by E. Eberlein and M. Taqqu (Birkhäuser, Boston, 1986), p. 137.
[22] P. Embrechts and M. Maejima, Int. J. Mod. Phys. B **14**, 1399 (2000); *Selfsimilar Processes* (Princeton University Press, Princeton, NJ, 2002).
[23] C. Tsallis, S. V. F. Levy, A. M. C. Souza, and R. Maynard, Phys. Rev. Lett. **75**, 3589 (1995); **77**, 5442 (1996).
[24] C. Tsallis, Phys. World **10**, 42 (1997).
[25] A. Janicki and A. Weron, *A Simulation and Chaotic Behaviour of α-Stable Stochastic Processes* (Dekker, New York, 1994).
[26] Sz. Mercik, K. Weron, K. Burnecki, and A. Weron, Acta Phys. Pol. B **34**, 3773 (2003).
[27] K. Burnecki, J. Rosiński, and A. Weron, in *Stochastic Processes & Related Topics*, edited by I. Karatzas, B. Rajput, and M. Taqqu (Birkhäuser, Boston, 1998), p. 1.
[28] H. E. Hurst, Trans. Am. Soc. Civ. Eng. **116**, 770 (1951).
[29] V. Klemes, Water Resour. Res. **10**, 675 (1974).
[30] J. Beran, *Statistics for Long-Memory Processes* (Chapman & Hall, New York, 1994).
[31] A. Montanari, M. S. Taqqu, and V. Teverovsky, Math. Comput. Modell. **29**, 217 (1999).
[32] Sz. Mercik, K. Weron, and Z. Siwy, Phys. Rev. E **60**, 7343 (1999); Sz. Mercik and K. Weron, *ibid.* **63**, 051910 (2001).
[33] Sz. Mercik and K. Weron, Acta Phys. Pol. B **5**, 1621 (2001).
[34] R. Weron, in *Empirical Science of Financial Fluctuations*, edited by H. Takayasu (Springer-Verlag, Tokyo, 2002), p. 110.
[35] A. M. Churilla *et al.*, Ann. Biomed. Eng. **24**, 99 (1996).
[36] C.-K. Peng *et al.*, Phys. Rev. E **49**, 1685 (1994).
[37] G. Samorodnitsky and M. S. Taqqu, *Stable Non-Gaussian Random Processes: Stochastic Models with Infinite Variance* (Chapman & Hall, London, 1994).
[38] R. Weron, Physica A **312**, 285 (2002).
[39] A. Zygmund, *Trigonometric Series*, 2nd ed. (Cambridge University Press, London, 1959).
[40] M. Maejima, Sugaku Expo. **2**, 102 (1989).
[41] K. Burnecki, Probab. Math. Stat. **20**, 261 (2000).
[42] K. Burnecki, M. Maejima, and A. Weron, Yokohama Math. J. **44**, 25 (1997); K. Burnecki and A. Weron, Acta Phys. Pol. B **35**, 1343 (2004).
[43] A. V. Chechkin and V. Yu. Gonchar, Physica A **277**, 312 (2000).
[44] T. Chang, T. Sauer, and S. J. Schiff, Chaos **5**, 376 (1995).

[45] T. Chang *et al.*, Biophys. J. **67**, 671 (1994).
[46] U. Krengel, *Ergodic Theorems* (De Gruyter, Berlin, 1985).
[47] J. Rosiński, Ann. Prob. **23**, 1163 (1995); **28**, 1797 (2001).
[48] Y. Kasahara, M. Maejima, and W. Vervaat, Stochastic Proc. Appl. **30**, 329 (1988).
[49] S. Cambanis, M. Maejima, and G. Samorodnitsky, Stochastic Proc. Appl. **42**, 91 (1992).
[50] D. Surgailis, J. Rosiński, V. Mandrekar, and S. Cambanis, Probab. Theory Relat. Fields **97**, 543 (1993).
[51] E. Gorczyńska *et al.*, Pfluegers Arch. **432**, 597 (1996).
[52] A. Fuliński *et al.*, Phys. Rev. E **58**, 919 (1998).
[53] http://www.earth.nasa.gov
[54] P. Varotsos, N. Sarlis, and E. Skordas, Proc. Jpn. Acad., Ser. B: Phys. Biol. Sci. **77**, 93 (2001).